2011 IEEE/RSJ International Conference on
Intelligent Robots and Systems
September 25-30, 2011. San Francisco, CA, USA

On the Convergence of Braitenberg Vehicle 3a immersed in Parabolic Stimuli

Iñaki Rañó*
*Institut für Neuroinformatik,
Ruhr-Universität-Bochum,
Germany

Abstract— **Braitenberg vehicles are well known models of animal behaviour prone to be used as a mobile robot controller. Due to the qualitative simplicity of their behaviour they are used for teaching robotics, whilst the lack of a quantitative theory makes its use for research purposes troublesome. This paper contributes to our formal understanding of Braitenberg vehicle 3a by presenting some convergence properties of its trajectories under parabolic shaped stimuli or potential functions. We show new features of the vehicle motion unreported in robotics like, their conditional stability, their oscillatory behaviour and the existence of a preferred convergence direction. Quantitatively identifying the behaviour of Braitenberg vehicles allows to use them in robotics on a sound basis, not just relying on incomplete qualitative understanding as done by earlier works.**

Index Terms— **Braitenberg Vehicles, Target reaching, Stability.**

I. Introduction

Braitenberg vehicles [3] qualitatively model sensor based animal steering and have long been used on an empirical basis on Artificial Life [17] [21] and robotics. The four most basic ones 2a/3b and 2b/3a model avoidance and target seeking behaviours respectively. One of their main usages in robotics teaching [4] [20] because they can be quickly understood qualitatively without any mathematical formulation. This greatly helps introducing robotics to youth as they can start playing around and experimenting with small robots without taking scaring mathematical courses, but also make researchers look down on Braitenberg vehicles as an amusement not as a research topic. This might be the reason why they are referred as the example on how complexity can emerge from simple interactions [9] [11], instead of an example of a biologically inspired sensor driven control system. Indeed, what the early vehicles of the book [3] model is animal motion towards, or escaping from, a stimulus, long known in biology as positive or negative taxis behaviour [6]. Animals are extremely good at moving in the real world and, therefore, they are a good model to follow when implementing robotic controllers. While positive taxis is a goal seeking technique, negative taxis implements avoidance behaviours, very common tasks on mobile robotics. Moreover, as these models work at the steering or guidance level they can be used with any locomotive configuration.

Different Braitenberg vehicles have been used to provide robots with several abilities on an experimental basis, and using a wide variety of stimulus, from light intensity to chemical concentration or even the free space in front of a robot as an artificial stimulus field or potential function. An implementation of target acquisition using vehicle 3a is presented in [2]. The robot performs phototaxis, motion towards light, in a combination with infrared based obstacle avoidance thought vehicle 2b. In fact, their low level version of the dynamical systems approach to behaviour generation [19] can be viewed as a Braitenberg vehicle where a stimulus is build up from infrared sensor readings. The infrared sensors provide an estimate of the distance to the objects around they want to avoid while advancing towards the light using the taxis behaviour. Inspired by the low level dynamical systems approach to behaviour generation, [16] presents a wandering mechanism, implemented on a big wheeled in-door robot, based on Braitenberg vehicle 2b for which an artificial stimulus was built up from laser and sonar proximity readings. The artificial function of the sensor readings is just a weighted integration of all the sensor values which provided an approximate of the free area in front of the robot. The wandering trajectories using this techniques are smooth, but this work was too simple as it lacked a purposive motion. However recent theoretical results and empirical evidences show wandering behaviour can be achieved through a Braitenberg vehicle 2b [13] [15]. Through fuzzy controllers, Braitenberg vehicles 3a and 2b are used for local navigation in [23]. Instead of generating direct velocity commands to the wheels they generate offset velocities, and therefore this makes it some kind of incremental, or higher order vehicle implementation. Goal seeking is achieved by vehicle 2b while vehicles 3b and 2a are used to avoid obstacles in the front and back of the robot respectively. A purely experimental analysis of vehicles 3a and 3b for odour source localisation is presented in [8], where the connection between sensors and motors is linear but sensor readings are normalised and averaged. Due to the nature of the stimulus and sensing hardware, there is a necessary sensor preprocessing that introduces a dynamic component on the connection, and therefore this is not a 3 type Braitenberg vehicle in a strict sense. Interestingly some of the trajectories look similar to simulations based on idealised stimulus [14] possibly pointing their dynamic sensing component can be neglected. Lego^{TM} technology is used to build Braitenberg vehicles, commonly wheeled robot [5] but also aquatic ones [20]. A simple Lego^{TM} hardware implementation of the vehicle 3b for obstacle avoidance, jointly with a wall following behaviour is presented in [5].

978-1-61284-456-5/11/$26.00 ©2011 IEEE

The power supply of the wheels is connected in a decreasing way to infrared sensors placed in the front of the robot, which makes the vehicle to slow down when objects are detected. Vehicles type 2 are implemented in aquatic robots, using Lego^{TM}, to approach or follow light sources as part of an early course on robotics [20]. This clearly shows that application of Braitenberg vehicles can be extended to other than wheeled robots.

The lack of formal techniques to understand and design Braitenberg vehicles made so far their implementation an educated guess based on empirical experience. A more complex way, we can find in the literature, of tuning their controllers is by applying neural networks or evolutive techniques. For instance, [22] presents a four neuron model of cricket phonotaxis, motion towards a sound source, built with spiking units. This model is comparable to the combination of vehicles 2a and 3b as excitatory units display a direct connection between sensors and motors, while inhibitory ones are crossed. Even the dynamic component of the neural network implies a non strict application of Braitenberg vehicles, the fast firing of the units relative to the vehicle dynamics low pass filters the sensor inputs. Inspired by Braitenberg's work too, [7] presents a foraging robot neural controller with neuromodulation, a change on the behaviour of neurons allowing a switch between vehicle types 2b and 3b. Evolution of Braitenberg vehicle 2b using genetic algorithms is presented in [10], where the evolved vehicles outperform free random evolution of agent morphology and control. They measure fitness in terms of a simulated reward, and find that half of the individuals actually converged to vehicle 3a. Another example of evolutive strategies applied to Braitenberg vehicles can be found in [18], where an initial random mixture of vehicles 3a and 3b is evolved on a Khepera robot to implement a wandering behaviour on a closed arena.

Despite all these robotics applications of Braitenberg vehicles for; target seeking, wandering, sound source localisation or obstacle avoidance, no formal theory allows to understand, predict or adjust their motion. Using these control mechanisms turns the implementation into a matter of trial and error through empirical comparison with the expected behaviour of the robot, a tedious task for the newcomer researcher on the area. This paper contributes to our understanding of Braitenberg vehicle 3a by presenting a mathematical analysis of their behaviour in the vicinity of parabolic stimulus or potential fields. Instead of relying on specific experimental data, we analyse the general non linear differential equations describing their behaviour, such that the results are valid for any application of vehicle 3b. New and unexpected results are presented that challenge our empirical understanding on how Braitenberg vehicle 3a behaves. The rest of the paper is organised as follows. Section II reviews the assumptions and the mathematical model derived for Braitenberg vehicle 3a. It also provides a set of theoretical results about the trajectories described under circular symmetric stimulus fields. Section III presents some analytic solutions of the non linear dynamical system describing vehicle 3a under a parabolic, non circularly symmetric, stimulus or potential field. With these solutions as an starting point further results on the trajectories are obtained. This section also presents simulations to illustrate the theoretical results. Finally, Section IV presents a summary of the conclusions and future steps on the development to a theoretical framework for Braitenberg vehicles.

II. Results for Circularly Symmetric Stimulus

A simple model for animal taxis is proposed for dual-drive wheeled vehicles in [3] as a thought experiment, a mental exercise without real world implementation. Figure 1 shows the vehicle 3a in the proximity of a light source, which represents a way of abstracting simple animals living in a worlds with different stimuli they can perceive. The wheels of the vehicle abstract animal locomotive subsystems, while allowing a general motion configuration with simple control mechanisms. In fact, similar steering models have been used to understand human motion [1]. The vehicle has two sensor placed in a biologically way that allow it to sense certain stimulus or scalar potential field. These sensors are connected, as shown in the figure, to a corresponding wheel in a decreasing way such that the stronger the stimulus or potential value the slowest the wheel turns. A fast intuition based analysis shows that the vehicle will turn towards the light source while approaching it. As it gets closer to the source, or maximum, it will slow down, and eventually, once it is close enough it might stop in front of it. Due to the intuitive convergence properties of the motion no further formalisation or analysis was performed even though they were used in real robots.

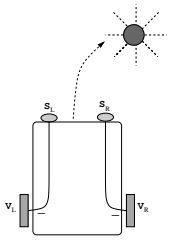

Fig. 1. Braitenberg vehicle 3a.

We will briefly review the modelling assumptions that lead to motion equations for vehicle 3a (see [14] for further details). The stimulus field can be modelled as a smooth scalar function of the position of the vehicle's workspace $S(\mathbf{x})$ for $\mathbf{x} = (x, y) \in \mathcal{W} \subseteq R^2$, and $S(\mathbf{x})$ is C^∞. If there is a single source or maximum, without loss of generality, we can set the origin of the a Cartesian coordinate system such that $S(\mathbf{0}) \geq S(\mathbf{x}) \forall \mathbf{x} = (x, y) \in \mathcal{W}$. This means the gradient of $S(\mathbf{x})$ vanishes at the origin while the Hessian matrix is negative definite, i.e. $\nabla S(\mathbf{0}) = \mathbf{0}$ and $\mathbf{y}^T D^2 S(\mathbf{0}) \mathbf{y} < 0 \forall \mathbf{y} \in R^2$. As the connection between the sensor readings s and the wheel velocities v is direct and decreasing, we can model it as a smooth decreasing function $F(s)$, such that $s \in \Re^+$, the stimulus is positive; $F(s) \geq 0$, the vehicle does not move backwards as it has no rear sensors and $F(s) = 0$ only at

the source maximum; and $F'(s) < 0$ since the connection is decreasing. Approximating the stimulus around the midpoint between the sensors of the vehicle we obtain the general motion equations for vehicle 3a:

$$\dot{x} = F(S(\mathbf{x}))\cos\theta \quad (1)$$

$$\dot{y} = F(S(\mathbf{x}))\sin\theta \quad (2)$$

$$\dot{\theta} = -\frac{\delta}{d}\nabla F(S(\mathbf{x}))\cdot\hat{e}_p \quad (3)$$

where δ is the distance between the sensors, d is the wheelbase of the vehicle and $\hat{e}_p = [-\sin\theta, \cos\theta]$.

If the stimulus function displays circular symmetry around the source, $S(\mathbf{x})$, and therefore $F(S(\mathbf{x}))$, can be expressed as a function of the distance to the origin. Therefore, we will write $F(S(r))$[1] where r is the polar coordinate of the vehicle, and obviously the gradient of $F(S(r))$ has only radial component. Using this simplifying assumption on the gradient, if we transform the system of differential equations (1), (2) and (3) to polar coordinates (r, ψ) the angular variables appear on the right hand side of the equations as the difference '$\psi - \theta$'. Defining a new variable $\eta = \psi - \theta$ we can write a simpler system of differential equations describing the motion of the Braitenberg vehicle 3a under circular symmetric stimuli as:

$$\dot{r} = F(r)\cos\eta \quad (4)$$

$$\dot{\eta} = -\left[\frac{F(r)}{r} - \frac{\delta}{d}\frac{\partial F(r)}{\partial r}\right]\sin\eta \quad (5)$$

where $F(r) = F(S(r))$ and η represents the vehicle heading relative to the polar angular coordinate. We can further define the discriminant function $G(r) = \frac{F(r)}{r} - \frac{\delta}{d}\frac{\partial F(r)}{\partial r}$ to analyse the general stability of this non-linear system of differential equations.

As for circularly symmetric stimuli there is no preferred angular direction we can analyse equations (4) and (5) which is a two dimensional, and easier to deal with, dynamical system instead of the three dimensional original one. One way of analyse the behaviour of the system, including stability properties, is to draw the phase plot, as done in figure 2, where the directions of the arrows show how the variables change for different regions of the phase plane. Even though the sign of the radial flow component depends only on $\cos\eta$, the sign of the angular component can change with the sign of the discriminant function. Figure 2(a) shows the flow vectors for a stable situation ($G(r) < 0$) where the vehicle moves towards the polar point $(0, \pi)$, the intuitively understood behaviour. On the other hand, if the discriminant function is positive $G(r) > 0$ the vehicle will end up moving away of the stimulus or potential minimum as shown in figure 2(b). The pathological case when $G(r) = 0$ for all r, which can be solved analytically, is not shown, but it corresponds to vehicles moving in logarithmic spiral

[1]This is a simplifying abuse of notation as the stimulus might have another functional form in polar coordinates.

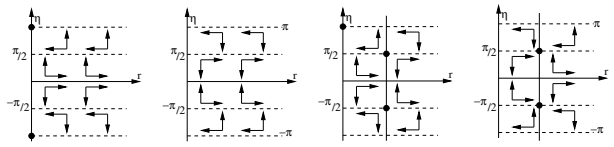

(a) $G(r) < 0$ (b) $G(r) > 0$ (c) Sign change 1 (d) Sign change 2

Fig. 2. Vector Flow sketch in reduced coordinates

trajectories toward or escaping from the source depending on their initial conditions. None of those two situations can be guessed easily from the intuitive understanding of Braitenberg vehicle 3a.

An even stranger situation can occur when the sign of $G(r)$ changes for different values of r, as shown in figures 2(c) and 2(d). While, for the flow corresponding to figure 2(c), any trajectory starting on the left side of the plane phase will converge to the point $(0, \pi)$, initial conditions on the right will diverge from the source leaving it straight behind. Two unstable periodic solutions appear at the intersection of the line defined by $G(r) = 0$ and $\theta = \pm\pi/2$ making the robot to turn around the source in clockwise and counter-clockwise directions. On the other hand, figure 2(c) shows a flow where these two parts of the phase plane are swapped, originating an attractor at the intersection of the line defined by $G(r) = 0$ and $\theta = \pm\pi/1$, and producing oscillatory trajectories close to it, i.e. the superposition of two oscillatory motions. Even though theoretically possible, tho the best knowledge of the author, this behaviour has never been reported before as the result of a Braitenberg vehicle 3a implementation or simulation. The analytical techniques used to compute the frequencies of motion and approximated trajectories for Braitenberg vehicle 2b [13] can also be used in this case.

III. Braitenberg vehicle 3a on Parabolic Stimuli Field

Results obtained so far are valid for circularly symmetric functions, which might not be always the case for some stimuli or potential. We will focus on the more complex situation of a function $S(\rho)$ where $\rho = \mathbf{x}^T\Sigma\mathbf{x}$, which is general enough as smooth stimuli can be approximated by such a function [12]. As we want $S(\mathbf{x})$ to be positive and to have a maximum at the origin we will assume Σ is a positive definite matrix, while $S(\rho)$ will be a positive and decreasing function of ρ with bounded derivative at $\rho = 0$. It is worth noting that this case includes the circularly symmetric situation when $\Sigma = I_{2\times 2}$, the identity matrix. Without loss of generality we can assume Σ is a diagonal matrix, which means the principal axes of the stimulus function coincide with the coordinate axes of the Cartesian coordinates. Under these condition the motion equations of the vehicle can be stated as:

$$\dot{x} = F(S(\rho))\cos\theta \quad (6)$$

$$\dot{y} = F(S(\rho))\sin\theta \quad (7)$$

$$\dot{\theta} = -2\frac{\delta}{d}F'(S(\rho))S'(\rho)\mathbf{x}^T\Sigma\hat{e}_p \quad (8)$$

where $F'(s)$ and $S'(\rho)$ represent the derivatives of the function w.r.t. s and ρ respectively.

We assumed the compound function $F(S(\rho))$ will vanish at the origin, $\rho = 0$, and equations (6) and (7) simultaneously vanish, while equation (8) vanishes too since $\rho = 0 \iff \mathbf{x} = \mathbf{0}$. This means the motion equations have an equilibrium point at the origin for parabolic shaped stimuli, and therefore a vehicle initially located at the source will stay there forever. However we are interested in the non-trivial case of the vehicle initial condition not being at the origin.

A. Analytic solutions of motion dynamics

Since Σ is a diagonal matrix, $diag(\Sigma) = (s_1, s_2)$, when equation (8) vanishes we find straight line trajectories of the vehicle. This translates into the condition $-xs_1\sin\theta + ys_2\cos\theta = 0$, which occurs when $x = 0$ and $\cos\theta = 0$ simultaneously, or $y = 0$ and $\sin\theta = 0$ simultaneously. As the trajectories must fulfil $x = 0$ or $y = 0$, they coincide with the principal axes of the stimulus function, which means any vehicle starting at the principal axis of the stimulus with the appropriated heading will move along a straight line.

As a case study, let us analyse the situation when the vehicle starts somewhere on the x Cartesian axis, i.e. $y_0 = 0$. The trajectory will be a straight line only if $\sin\theta_0 = 0$, which makes vanish equations (7) and (8) simultaneously. The vehicle motion is described by the solution to $\dot{x} = \pm F(S(s_1x^2))$, and the sign depends on whether $\theta_0 = 0$ or $\theta_0 = \pi$, giving two possible vehicle behaviours. It is worth reminding that, $F(S(\mathbf{x})) \geq 0$ and the identity only occurs for $\mathbf{x} = \mathbf{0}$, which means the origin is an equilibrium point. However, the linear stability test does not work for the equation at hand. Moreover, the non linear differential equation describing the motion of vehicle 3a is conditionally stable as shown in figure 3. According to figure 3(a), when the initial heading of the vehicle is $\theta_0 = 0$ the equilibrium point at the origin is an attractor for initial conditions $x_0 < 0$, and a repellor for $x_0 > 0$. The interpretation of this result is straightforward, when the vehicle heads the source from a negative position it will move in a straight line approaching the origin. However, if the source falls exactly behind the vehicle, as the stimulus perceived in both sensors is identical, the vehicle will move forward without turning, leaving the origin exactly at its back. Therefore, this time the theoretical result clearly matches our intuition on how Braitenberg vehicle 3a works. A similar analysis can be performed for the initial condition $\theta_0 = \pi$, however the flow points in the opposite direction as shown in figure 3(b).

In sum, we found several analytic solutions to the motion equations of the Braitenberg vehicle 3a. The simplest case is the vehicle starting condition being the stimulus maximum point, which produces the trivial "no motion" trajectory.

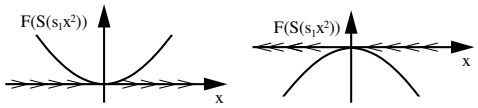

(a) $\theta_0 = 0$ (b) $\theta_0 = \pi$

Fig. 3. Stability of the motion equations along the x axis.

When the vehicle initial conditions lay on the principal axis of the stimulus function and the heading points to the source, or in the opposite direction, the trajectories are straight lines towards the source, or moving away from it. This later case matches previous results for circular symmetric stimuli [12] where any direction is a principal axis of the stimulus, and therefore all trajectories pointing to the source follow a straight line. Moreover, we proved that, at least for the principal axes of the stimulus, the vehicle pointing in the appropriate direction at the right side of the source, the origin is a stable equilibrium point, and therefore it will attract the vehicle. Now the questions arise, is the maximum of the stimulus always an attractor? which kind of trajectories does the vehicle show when approaching the origin? This questions have been apparently reported in the many experimental uses of Braitenberg vehicle 3a, but as we will see in the next section theoretical results challenge our intuitive understanding once more.

B. Approximated trajectories close to the principal axes

Finding non equilibrium analytic solutions to non linear dynamical systems is not common, but it is very useful as it allows to analyse the solution trajectories in the vicinity of the analytic one. The tool used under these circumstances is linearisation of the dynamical system around the trajectory, which for the case of an equilibrium point allows to derive the linear stability test. The first step to proceed with the analysis is to obtain the Jacobian matrix of the equations (1), (2) and (3), which can be stated as:

$$J = \begin{bmatrix} \nabla F(S(\mathbf{x}))\hat{e}^T & F(S(\mathbf{x}))\hat{e}_p^T \\ -\frac{\delta}{d}\nabla_{x|y}F(S(\mathbf{x}))^T\hat{e}_p & \frac{\delta}{d}\nabla F(S(\mathbf{x}))^T\hat{e} \end{bmatrix} \quad (9)$$

where $\nabla F(S(\mathbf{x}))\hat{e}^T$ is the 2×2 matrix resulting from the product of the gradient of $F(S(\mathbf{x}))$ and the heading unit vector of the vehicle $\hat{e} = [\cos\theta, \sin\theta]$, $F(S(\mathbf{x}))\hat{e}_p^T$ is the vector orthogonal to the vehicle direction scaled by its linear velocity, $\frac{\delta}{d}\nabla_{x|y}F(S(\mathbf{x}))^T\hat{e}_p$ is a 1×2 matrix formed by second order cross derivatives of $F(S(\mathbf{x}))$, and $\nabla F(S(\mathbf{x}))^T\hat{e}$ is the directional derivative of $F(S(\mathbf{x}))$ along the vehicle heading. This matrix has to be evaluated at the trajectory to obtain the behaviour of nearby trajectories. Specifically, the linear trajectory can be stated as; $y_l(t) = 0$, $\theta_l(t) = 0$ (or $\theta_l(t) = \pi$) and $x_l(t)$ is the solution of $\dot{x} = F(S(s_1x^2))$. If we use this solution with equation (9), taking the case $\theta_l(t) = 0$, the resulting matrix is:

$$J = \begin{bmatrix} 2F'S's_1x & 0 & 0 \\ 0 & 0 & F(S(s_1x^2)) \\ 0 & -2\frac{\delta}{d}F'S's_2 & 2\frac{\delta}{d}F'S's_1x \end{bmatrix} \quad (10)$$

where $F' = F'(S(s_1x^2))$ and $S' = S'(s_1x^2)$ are the derivatives of $F(s)$ and $S(\rho)$ w.r.t. their arguments along the trajectory $x_l(t)$ respectively. Any trajectory starting close to the solution will be a linear combination of the straight line trajectory and the solution to the system of differential equations defined by the Jacobian matrix (10), which is a linear time dependent dynamical system. Moreover, we can compute the eigenvalues of the above matrix to check whether close trajectories to the analytical solution converge to it or diverge. The eigenvalues λ_i for the case $\theta_l(t) = 0$ are

$$\begin{aligned} \lambda_1 &= 2s_1xF'S' \\ \lambda_{2,3} &= \frac{\delta}{d}s_1xF'S' \mp \sqrt{\left(\frac{\delta}{d}s_1xF'S'\right)^2 - 2\frac{\delta}{d}F'S'Fs_2} \end{aligned}$$

where $F = F(S(s_1x^2))$ is evaluated along $x_l(t)$.

According to our assumptions $S(\rho)$ should have a maximum at the origin or stimulus source, therefore it is a decreasing function $S'(\rho) < 0$. The connecting function $F(s)$ for Braitenberg vehicle 3a is also decreasing $F'(s) < 0$, and the matrix Σ is positive definite, therefore $s_1 > 0$ and $s_2 > 0$. Having all this in mind, we can see the sign of the first eigenvalue $\lambda_1 = 2F'S's_1x$ depends on the value of x. Moreover, since $F'S's_1 > 0$ the trajectories of the linearised system will diverge from the straight line trajectory when $x > 0$, as the eigenvalue is positive. This again matches our intuition on how Braitenberg vehicle 3a behaves. We saw that the vehicle with the initial conditions $\theta_0 = 0$, $y_0 = 0$ and $x_0 > 0$ will move away from the source following the principal stimulus axis. However, if θ_0 or y_0 are not exactly zero, it will start turning to head the source and therefore its trajectory will diverge from the stimulus principal axis. It is worth noting that the second and third eigenvalues will produce the same effect as they share the same term, while the part inside the square root will always have an absolute value smaller than the former. Therefore, all the eigenvalues have the same sign and the vehicle will move away from the straight line trajectory.

On the other hand, when $x < 0$ all the eigenvalues are negative, hence any trajectory starting close to the analytic solution will get closer to it. That again matches our intuition of what happens when the vehicle starts from a position that roughly heads the stimulus source along the principal axes, it will move towards it. However, a special, and previously unreported, situation can happen if the term inside the square root is negative, because the two eigenvalues $\lambda_{2/3}$ will be complex numbers. What the equations say is that oscillatory behaviour should be displayed by these vehicles close enough to the origin. The specific condition when this occurs is $\frac{\delta}{d}F'S's_1^2x^2 - 2Fs_2 < 0$, which might be fulfilled for certain x value as the vehicle approaches the source. We can see that the distance for which oscillations around the principal stimulus axis occurs depends, among other factors, on the relation between s_2 and s_1. Similar results can be obtained if the trajectories are analysed around the other analytic solution, $x_l(t) = 0$, $\theta_l(t) = \pm\pi$ and $\dot{y} = F(S(s_2y^2))$, but the roles of s_1 and s_2 are exchanged.

C. Simulated Results

To illustrate the oscillatory behaviour for non symmetric stimulus sources we integrated the motion equations under a stimulus field for $s_1 = 1$ and different s_2 values. On the one hand, it is worth noting that this is a general enough setting, since values of $s_1 \neq 1$ can be codified inside the derivative of the function $S(\rho)$ with the proper scaling of s_2. On the other hand, it is worth reminding stimulus coming from a source with a non-isotropic emission pattern can be always approximated close to the source as a parabolic function. In order to compare the results with the symmetric trajectory we plot the simulation corresponding to $s_2 = 1$. All the simulations are run using a fixed step ($h = 0.01$) fourth order Runge-Kutta algorithm.

Figure 4(a) shows the trajectories for $s_2 = \{1, 5, 10\}$ with initial conditions close to the principal axis $y = 0$, specifically $(x_0, y_0, \theta_0) = (4, 0.2, 0)$. Since $s_2 > s_1$ oscillations appear around the x axis, earlier as s_2 increases relative to s_1. Because λ_1 is always negative and $\lambda_{2/3}$ have negative real part, the amplitude of oscillations decreases exponentially as a first order approximation. This exponential modulation could make the oscillatory effect negligible in real vehicle applications. We also see that the frequency of the oscillations increases as the vehicle approaches the stimulus maximum. This results from the eigenvalues being actually a function of the vehicle x coordinate, i.e. the approximated linear system is time dependant. To the best of our knowledge, this oscillatory behaviour has not been reported on any of the experimental works using Braitenberg vehicle 3a, probably because the parameters on the controller function $F(s)$ are experimentally tuned to avoid this situation. This can be adjusted by choosing the right $F(s)$ since if its value decreases fast enough, the term inside the square root of the eigenvalues $\lambda_{2/3}$ could be positive and no oscillation will appear.

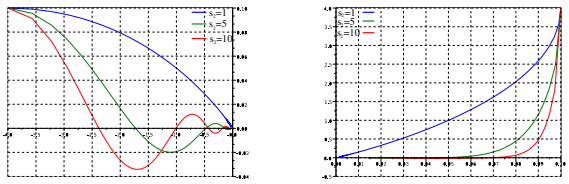

(a) Oscillatory behaviour for non-symmetric stimulus. (b) Non oscillatory behaviour around the orthogonal direction.

Fig. 4. Trajectories close to the analytic solution.

Figure 4(b) shows the trajectories of the vehicle with initial

conditions close to the complementary axis $(x_0, y_0, \theta_0) = (0.1, 4, -\pi/2)$ using the same s_1 and s_2 values. As the figure shows, trajectories quickly turn towards the x axis with an increasing strength as the value s_2 increases, and despite the figure scale does not allow to see it, in the end, the trajectory oscillates around the x axis. From the figure, it seems there is a preferred direction for the vehicles to approach the origin, but the simulation can be misleading since the initial angular direction is already parallel to the y axis.

To really test whether there is a preferred approaching direction we performed the simulations presented in figures 5(a) and 5(b). Figure 5(a) shows a simulations with initial conditions $(x_0, y_0, \theta_0) = (-2, 2, -\pi/4)$, corresponding to a straight line trajectory for the symmetric case $s_1 = s_2 = 1$, and since the initial conditions are equidistant to both axes, both approximations are equally valid. The figure shows how the trajectories for $s_2 \neq 1$ actually approach along the x axis, the one with the smallest curvature, i.e. Braitenberg vehicles 3a approach a parabolic potential minima along the principal axis which has the minimum curvature. Figure 5(b) shows the same effect for five random initial conditions of the vehicle immersed in a parabolic stimulus with principal axes not aligned to the Cartesian coordinates. This figure shows too this same effect which can be used to force the vehicle to reach a point in a preferred direction by properly design an artificial stimulus field.

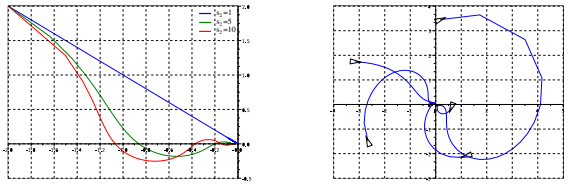

(a) Equidistant approximation (b) Random simulations

Fig. 5. Preferred approach direction for parabolic stimuli.

IV. Conclusions and Further Work

This paper contributes to the theoretical understanding of Braitenberg vehicle 3a, a qualitative model of animal steering control for goal seeking, while previous works were purely based on experimental results. Contrary to the intuitive understanding of Braitenberg vehicle 3a, we were able to theoretically predict the existence of unstable configurations, or periodic trajectories around the stimulus source even for the simple case of circular symmetry. When the symmetry condition is not fulfilled we proved some straight line trajectories exist that allows us to analyse the behaviour of the vehicle and test for a preferred approach direction to the target source. In sum, this work provides an analysis of the convergence properties of a biologically inspired steering control mechanism for non-holonomic, unicycle, motion configurations.

Since most of the performed research on Braitenberg vehicles has been mainly experimental, future work mandates keeping the track of a theoretical approach. So far we assumed the stimulus function is strictly non increasing, however it might be interesting to be able to compensate a local maximum on the stimulus function through the internal control function $F(s)$, whenever it is possible, to speed up the convergence. This involves finding a non empirical mechanism to design Braitenberg vehicles for complex configurations, potentially avoiding oscillatory behaviour or specifying an approach direction to the target.

References

[1] G. Arechavaleta, J. P. Laumond, H. Hicheur, and A. Berthoz. An optimality principle governing human walking. *IEEE Transactions on Robotics*, 24(1):5–14, 2008.

[2] E. Bicho and G. Schöner. The dynamic approach to autonomous robotics demonstrated on a low-level vehicle platform. *Robotics and Autonomous Systems*, 21:23–35, 1997.

[3] V. Braitenberg. *Vehicles. Experiments in synthetic psychology*. The MIT Press, 1984.

[4] C. Buiu. Hybrid educational strategy for a laboratory course on cognitive robotics. *IEEE Transactions on Education*, 51(1):100–107, 2008.

[5] L. Capozzo, G. Attolico, and G. Cicirelli. Building low cost vehicles for simple reactive behaviors. In *Proceedings of the IEEE International Conference on Systems, Man, and Cybernetics*, volume 6, pages 675–680, 1999.

[6] G.S. Fraenkel and D.L. Gunn. *The orientation of animals. Kineses, taxes and compass reactions*. Dover publications, 1961.

[7] R.L.B. French and L. Cañamero. Introducing neuromodulation to a Braitenberg vehicle. In *Proceedings of the 2005 IEEE International Conference on Robotics and Automation*, pages 4188–4193, 2005.

[8] A. J. Lilienthal and T. Duckett. Experimental analysis of gas-sensitive Braitenberg vehicles. *Advanced Robotics*, 18(8):817–834, 2004.

[9] P. Maes. Modeling adaptive autonomous agents. *Artificial Life*, 1(1-2):135–162, 1994.

[10] C. Mautner and R. K. Belew. Evolving robot morphology and control. *Artificial Life and Robotics*, 4:130–136, 2000.

[11] R. Pfeifer. Building fungus eaters: Design principles of autonomous agents. In *Proceedings of the Fourth International Conference on Simulation of Adaptive Behavior*, pages 3–12. MIT Press, 1996.

[12] I. Rañó. On taxis for control and its qualitative solution on mobile robots. In *Proceedings of the Intelligent Autonomous Vehicles*, 2007.

[13] I. Rañó. Hanging around and wandering on mobile robots with a unique controller. In *Proceedings of the ECMR*, 2009.

[14] I. Rañó. A steering taxis model and the qualitative analysis of its trajectories. *Adaptive Behavior*, 17(3):197–211, 2009.

[15] I. Rañó. *An empirical evidence of Braitenberg vehicle 2b behaving as a billiard ball*, pages 293–302. Springer, 2010.

[16] I. Rañó and T. Smithers. Obstacle avoidance through Braitenberg's aggression behavior and motor fusion. In *Proc. of the 2nd European Conf. on Mobile Robots*, pages 98–103, 2005.

[17] M. Resnik. LEGO, Logo and Life. In *Artificial Life. Proceedings of an Interdisciplinary Workshop on the Synthesis and Simulation of Living Systems*, pages 397–406, 1987.

[18] R. Salomon. Evolving and optimizing Braitenberg vehicles by means of evolution strategies. *Int. J. Smart Eng. Syst. Design*, 2:6977, 1999.

[19] G. Schöner, M. Dose, and C. Engels. Dynamics of behavior: theory and applications for autonomous robot architectures. *Robotics and Autonomous Systems*, 16:213–245, 1995.

[20] R. Stolkin, R. Sheryll, and L. Hotaling. Braitenbergian experiments with simple aquatic robots. 2007.

[21] M. Travers. Animal construction kits. In *Artificial Life. Proceedings of an Interdisciplinary Workshop on the Synthesis and Simulation of Living Systems*, pages 421–442, 1987.

[22] B. Webb. *A Spiking Neuron Controller for Robot Phonotaxis*, pages 3–20. The MIT/AAAI Press, 2001.

[23] X. Yang, R. V. Patel, and M. Moallem. A Fuzzy-Braitenberg Navigation Strategy for Differential Drive Mobile Robots. *Journal of Intelligent Robotic Systems*, 47:101–124, 2006.